Am J Transl Res 2015;7(4):654-669
www.ajtr.org /ISSN:1943-8141/AJTR0003949

Original Article

Effects of thrombin and thrombin receptor activation on cardiac function after acute myocardial infarction

Xinyuan Gu[1,2*], Xiaorong Zhang[3*], Guihua Lu[4*], Yanhui Li[5], Xiujuan Li[6], He Huang[1], Jianping Zeng[1], Lilong Tang[1]

[1]Division of Cardiology, Xiangtan Central Hospital, Xiangtan, China; [2]Division of Cardiology, Yuebei Remin Hospital Affiliated to Medical College of Shantou University, Shaoguan, China; [3]Cerebropathia Department, Gansu Province Hospital of TCM Lanzhou, Gansu, China; [4]Division of Cardiology, The First Aaffiliated Hospital of Sun Yat-Sen University Guangzhou, China; [5]Department of Internal Medicine, Tongji Hospital, Huazhong University of Science and Technology Wuhan, China; [6]Department of Laboratory Medicine, Jiangmen Central Hospital Jiangmen, China. [*]Equal contributors.

Received November 18, 2014; Accepted April 11, 2015; Epub April 15, 2015; Published April 30, 2015

Abstract: Thrombin and thrombin receptor activation impact cardiomyocyte contraction and ventricular remodeling. However, there is some controversy regarding their effects in cardiac function, especially in cardiac dysfunction after acute myocardial infarction (AMI). A rat AMI model was created by left coronary artery ligation (LCA). Cardiac functional parameters, including the maximum left ventricular (LV) systolic pressure ($LVSP_{max}$), LV end-diastolic pressure (LVEDP), and the rise and fall rates in LV pressure (dp/dt_{max} and dp/dt_{min}, respectively), were measured. Hirudin decreased cardiac function within 120 minutes after AMI, whereas treatment with thrombin receptor-activating peptide (TRAP) reversed this hirudin-induced decrease in cardiac function. The mRNA and protein expression levels of inositol 1,4,5-trisphosphate receptor (IP_3R) subtypes in infarct area tissues were analyzed by reverse transcription-polymerase chain reaction and immunoreaction. Hirudin decreased the expression levels of IP_3R-1, -2, and -3 in the infarct area for up to 40 minutes after AMI, whereas TRAP treatment reversed these hirudin-induced effects. Treatment with the IP_3R antagonist 2-aminoethoxydiphenyl borate (2.5 mg/kg) eliminated the effect of TRAP on the hirudin-induced decrease in cardiac function after AMI. Finally, TRAP increased the maximum binding capacity of the three IP_3R subtypes, but only enhanced the affinity of IP_3R-2. Thrombin and thrombin receptor activation improved cardiac function after AMI by an IP_3R-mediated pathway, probably through the IP_3R-2 subtype.

Keywords: Thrombin, thrombin receptor, acute myocardial infarction, cardiac function, IP_3 receptor

Introduction

Cardiogenic shock occurs in ~7% of patients with acute myocardial infarction (AMI) [1, 2] and is responsible for most cases of early mortality after myocardial infarction [3]. Cardiogenic shock complicating AMI remains an important clinical problem, despite advances in reperfusion therapy. Activation of the sympathetic nervous system and various neurohumoral regulatory mechanisms protect cardiac function during the acute stress period after AMI. However, other potential protection mechanisms after AMI have not been fully explored.

Thrombin formation plays an important role in the course of AMI. In addition to participating in platelet aggregation, thrombin activates cells through its receptor, impacting a wide range of physiological systems, such as the endothelial barrier, chemotaxis, inflammation, cell growth and division, cardiomyocyte contraction, ventricular remodeling, and so on [4, 5]. Administration of thrombin receptor-activating peptide (TRAP) to mice *in vivo* caused rapid hypotension, followed by sustained moderated hypotension [6]. However, in thrombin receptor-deficient mice, the parameters of cardiac function and blood pressure (BP) were not different from levels in normal mice [7]. Therefore, there is some controversy regarding the role that thrombin plays in cardiac function.

The inositol 1,4,5-trisphosphate (IP_3) receptor (IP_3R) is present in the sarcoplasmic reticulum (SR) of cardiomyocytes. When combined with

IP_3, IP_3R can enhance cardiac contractile function through Ca^{2+} outflow from the SR [8]. Thrombin demonstrated a positive inotropic effect on rat myocytes *in vitro*, through a process involving increased cytosolic Ca^{2+} concentration in myocytes [9]. Thrombin receptor expression was increased after AMI within the ischemic myocardial tissue, but it is still unknown whether this expression will change the level of IP_3R and influence the cardiac function.

We previously demonstrated that thrombin and thrombin receptor activation can induce ventricular arrhythmia and ST-segment elevation after AMI [10, 11]. The aim of the present study was to clarify whether thrombin receptor activation affects cardiac systolic function *via* the IP_3 pathway after AMI.

Materials and methods

Materials

Hirudin was purchased from Fudan University (Shanghai, China). Evans blue and TRAP were purchased from Sigma Chemical Co. (St. Louis, USA). TRAP was dissolved in 0.1% trifluoroacetic acid (TFA; Sigma Chemical Co.) as a stock solution, and diluted in 0.005% TFA to a 250-nM working solution. Hirudin was dissolved in a working solution of 0.01% mannitol (final concentration). The IP_3R antagonist, 2-aminoethoxydiphenyl borate (2-APB; Sigma Chemical Co.), was prepared for intravenous (*i.v.*) injection by reconstitution in dimethyl sulfoxide (DMSO; Sigma Chemical Co.) and diluted in normal saline to achieve a final concentration of 10% DMSO [12]. Animals received 2.5 mg/kg 2-APB injected directly into the iliac vein in a total of 0.5 ml of normal saline.

Animal model

All experimental protocols complied with the Guide for the Care and Use of Laboratory Animals published by the US National Institutes of Health (NIH) and the Animal Care and Use Committees of Sun Yat-sen University. Sprague-Dawley rats (male, 200-250 g) were used for all experiments. The rat AMI model was created as described previously [10, 11]. Briefly, each rat was anesthetized with an intraperitoneal injection of ketamine/xylazine (75/5 mg/kg), intubated, and ventilated on room air throughout the procedure. Under sterile conditions, a left thoracotomy was performed at the third intercostal space. The pericardium was opened, exposing the left atrial appendage and pulmonary cone in the heart. Gentle pressure was applied on the right side of the thorax to provide quick access to the heart. A suture was placed under the left coronary artery (LCA) between the pulmonary artery outflow tract and the left atrium. If the ST segment in lead I was elevated upon tightening of the suture but returned to normal when the suture was relaxed, then the suture was tightened and tied using a 6-0 sterile silk 5 minutes after *i.v.* administration. The animal model of AMI was considered successful if: 1) the color of the infarcted area changed from red to white, 2) the left atrium was enlarged just after the coronary artery was ligated, and 3) the ST segment was elevated by more than 0.2 mm after LCA ligation. Myocardial ischemia was confirmed by the presence of regional cyanosis and ST segment elevation on the ECG. It was further confirmed by Evans blue perfusion after every experiment.

Sham-operated rats served as controls. All rats were euthanized after the experiments by anesthetization with 100% O_2/5% isoflurane, followed by either decapitation or transcardial perfusion with 0.9% saline containing 4% formaldehyde, depending on the protocol.

Measurement of cardiac function

For left ventricular (LV) cannulation, all animals were adequately anesthetized, intubated in a supine position, and ventilated on room air with a small animal ventilator. To find the common carotid artery (CCA), the right CCA sheath was separated continuously, and the vagus nerve was freed. An attempt was made to insert the tube into the LV *via* the CCA. The LV pressure was monitored by the tube. If the LV diastolic BP rapidly fell to near zero, then the tube was considered to have entered the LV.

After the tube was fixed, it was connected to a tension transducer and the BL-420 biological function experimental system (Chengdu Taimeng Technology Co, Ltd. China). Hemodynamic parameters of the LV, including the LV systolic pressure ($LVSP_{max}$), LV end-diastolic pressure (LVEDP), and the rise and fall rates in the LV pressure (dp/dt_{max} and dp/dt_{min}, respectively), were obtained. Cardiac functional parameters were consecutively recorded within 2 hours, at

1 minute before and after intervention, and 1, 5, 10, 20, 40, 80, and 120 minutes after LCA ligation.

To prevent blood from clotting in the tube, before each data point was recorded, the tube was washed with 200 μl of low-concentration heparin solution (12,500 U heparin in 500 ml of saline) for 5 seconds. To determine the cardiac functional parameters, each segment constituted 20 waves, with a 10-second interval between segments. For each time point, the average of three segments was used to determine the average cardiac functional parameter.

qRT-PCR analysis of IP_3R in the local infarct tissue

Myocardial tissue (100 mg) was cleaned with sterilized double-distilled water containing 0.1% diethylpyrocarbonate (DEPC). The tissue was homogenized with 1 ml of Trizol reagent, followed by extraction with chloroform. RNA was precipitated with isopropanol, washed with 75% ethanol, mixed in 40 μl of DEPC-containing water, and stored at -80°C until use. RNA extracted from the myocardial tissue was subjected to agarose gel electrophoresis. A ThermoScientific NanoDrop 1000 spectrophotometer was used to quantify RNA and assess RNA purity.

Total RNA (1 μg) was reverse-transcribed into cDNA with a cDNA synthesis kit (Invitrogen). The cDNA levels of IP_3R and β-actin (as a housekeeping gene) in the local infarct tissues were quantified by real-time PCR using the ABI PRISM 7700 Sequence Detection System (Applied Biosystems) with the DyNAmoTM ColorFlash® SYBR Green qPCR kit (Finnzymes Oy, Espoo, Finland). The PCR protocol consisted of an initial step at 95°C for 5 minutes, followed by 95°C for 10 seconds, 55°C annealing for 20 seconds, and establishment of a melting curve from 65 to 9°C.

Expression levels were calculated *via* the comparative threshold cycle (CT) method and normalized to the expression of human β-actin (as a housekeeping gene). ΔΔCt was used to calculate the fold change in mRNA expression, as follows: ΔCt = Ct (target gene) - Ct (housekeeping gene), ΔΔCt = ΔCt (treatment) - ΔCt (control), where fold change = $2 - (\Delta Ct_{sample} - \Delta Ct_{control})$. The primers used were as follows: for IP_3R-1, 5'-CGGAGTAGGA GATGTGCTCA G-3' and 5'-CATCTCTGCC ACGTAGCTCT C-3' (GenBank NM_001007235.1; 7967-7987 and 8304-8324); for IP_3R-2, 5'-CTCTCTGGCC TCCAGATTCT T-3' and 5'-GGTCCTAGTG TGTGCAGCAT T-3' (GenBank NM_031046.3; 9559-9579 and 9800-9820); for IP_3R-3, 5'-AGCACTACAT TGTGGCTGTC C-3' and 5'-AGAGAAAGTC CTGGGAGCAA G-3' (GenBank NM_013138.1; 8463-8473 and 8637-8657); and for β-actin, 5'-CACGGCATTG TCACCAACTG -3' and 5'-AGGGCAACAT AGCACAGCTT -3' (GenBank NM_031144.2; 298-317 and 724-743).

Immunoblotting of IP_3R in the infarct area

At every time point in each group, the heart was cut, and the atrium and right ventricle were removed. The pale (infarcted) areas were frozen at -80°C. Tissues were grinded with liquid nitrogen while being washed with 1 × PBS. Radioimmunoprecipitation lysis buffer, consisting of 25 mM Tris-HCl (pH 7.6), 150 mM NaCl, 1% NP-40, 1% sodium deoxycholate, and 0.1% sodium dodecyl sulfate (SDS), was added to lyse the tissue. Aprotinin, pepstatin, leupeptin, and phenylmethylsulfonyl fluoride (PMSF) were added to inhibit protein decomposition. The tissue was homogenized completely and placed on ice for 30 minutes to complete the lysis process. The sample was centrifuged at 4°C and 15,000 × *g* for 20 minutes. The supernatant was mixed with 5 × loading buffer, consisting of 0.25 M Tris-HCl (pH 6.8), 15% SDS, 50% glycerol, 25% β-mercaptoethanol, and 0.01% bromophenol blue. It was heated for 5 minutes at 100°C and centrifuged at 4°C and 12000 × *g* for 5 minutes. Proteins (30 μg/lane) were separated by four 15% gradient SDS-polyacrylamide gels and transferred to polyvinylidene difluoride membranes with a Mini Trans Blot Cell (Bio-Rad, Hercules, CA).

Membranes were incubated with polyclonal anti-IP_3R-1 (1:1,000 dilution), anti-IP_3R-2 (1:500 dilution), or monoclonal anti-IP_3R-3 (1:500 dilution; all Santa Cruz Biotechnology, TX) antibodies overnight at 4°C in Tris-buffered solution (TBS) with 0.1% Tween 20 (TBS-T) and 5% nonfat dry milk. After 3 washes with TBS-T, membranes were incubated for 1 hour with horseradish peroxidase (HP)-conjugated secondary antibody (1:10,000 dilution; Pierce Biotechnology) and washed with TBS-T. Membranes were developed using enhanced chemiluminescence (Amersham, Arlington Heights,

IL). They were reprobed with monoclonal anti-actin antibody (1:10,000 dilution; Chemicon International), followed by HP-conjugated anti-mouse IgG. Band intensities were quantified by digital densitometry using Quantity One version 4.4.1 software. The IP_3R isoform band intensity was normalized to β-actin.

Preparation of cardiomyocytes

Ventricular cardiomyocytes were isolated from rats (200-250 g) using a modification of a previously described method [1, 10]. Briefly, hearts were rapidly excised, cannulated, and subjected to retrograde perfusion on a Langendorff apparatus with Krebs-Henseleit (KH) buffer (in mmol/l: 10 HEPES, 118 NaCl, 4.7 KCl, 1.2 $MgSO_4$, 1.2 KH_2PO_4, 25 $NaHCO_3$, 11 glucose, and 1 $CaCl_2$; pH 7.37) for 2 minutes. They were perfused with Ca^{2+}-free KH buffer for 2 minutes, followed by Ca^{2+}-free KH buffer containing 0.5 mg/ml collagenase type II and 1 mg/ml bovine serum albumin (BSA) for 25 minutes. The LV was removed, chopped into small pieces, and incubated in a 50-ml Falcon tube at 37°C for 3 minutes with shaking. Undigested tissue was allowed to settle for ~1 minute. The pellet containing undigested tissue was discarded, and the Ca^{2+} concentration in the supernatant was gradually increased to 1.2 mmol/l.

Isolated cardiomyocytes were pelleted by centrifugation at 50 × *g* for 2 minutes at room temperature and resuspended in a stabilizing buffer (in mmol/l: 20 HEPES, 137 NaCl, 4.9 KCl, 1.2 $MgSO_4$, 15 glucose, and 1.2 Ca^{2+}; pH 7.4). The cell preparation was incubated in stabilizing buffer containing 1% BSA for ~15 minutes at 37°C. It was washed and resuspended in Medium 199 (Invitrogen, Guangzhou, China), supplemented with 100 IU/ml penicillin and 100 μg/ml streptomycin. This technique routinely yields 90% cardiomyocytes retaining a rod-shaped morphology [10, 11]. Experiments were performed on the same day or 4 hours after isolation.

Purification of IP_3R subtypes 1, 2, and 3 from cardiomyocytes

Cardiomyocytes were incubated with TRAP (250 nM) or 0.1% TFA for 30 minutes. The supernatant was removed, and the cells were rinsed once with Hank's Balanced Salt Solution (in mmol/l: 155 NaCl, 10 HEPES, and 1 EDTA; pH 7.4). The cells were placed on ice, and 3 to 6 ml of ice-cold lysis buffer (in mmol/l: 50 Tris-base, 150 NaCl, 1% Triton X-100, 1 EDTA, 0.2 PMSF, 1 dithiothreitol, 10 leupeptin, 10 pepstatin, and 0.2 soybean trypsin inhibitor; pH 8.0) were added to each dish. The cells were incubated for 30 minutes on ice and centrifuged at 10,000 × *g* for 20 minutes at 4°C. Supernatants in each dish were incubated at 4°C with polyclonal anti-IP_3R-1, -2, or -3 (1:40 dilution) and Agarose A/G beads (15 μl). They were resupinated overnight. Immune complexes were isolated by centrifugation at 10,000 × *g* for 2 minutes, and washed twice with lysis buffer. Finally, the washed beads were resuspended in 1.6 ml of 20 mM Tris-base and 1 mM EDTA at pH 8.0.

IP_3 binding to immunoprecipitated receptors

The Protein A bead/ antibody/ IP_3R complex was previously shown to remain intact during radioligand-binding studies [13, 14]. Thus, washed beads (100 ml) were incubated at 4°C for 30 minutes with $[^3H]IP_3$ (specific activity, 2-5 Ci/mmol Amersham Pharmacia Bio, UK) in 35 mmol/l Tris-base and 1.5 mmol/l EDTA, pH 8.0 (final volume, 200 ml). Bound ligand was isolated by vacuum filtration. Incubated mixtures were pipetted onto pre-moistured Whatman GF/B filters (Whatman Corp., UK) and washed twice with 4 ml of ice-cold 20 mmol/l Tris-base and 1 mmol/l EDTA, pH 8.0. Filters were added to vials with 0.5 ml of water and 5 ml of Ecoscint H. They were assessed for radioactivity after a 48-hour extraction.

Nonspecific binding was determined by including 10 μmol/l nonradioactive IP_3 in parallel incubations. Specific binding was analyzed with Prism (Packard Tri-Carb 2900TR, GMI, Inc., Meriden, CT, USA). Initially, the data were fitted to sigmoid curves of variable slope to determine the concentrations that gave half-maximal saturation. The maximum number of binding sites (B_{max}) obtained from these analyses was used to normalize data. Values of the equilibrium dissociation constant K_d for preparations of receptor types 1, 2, and 3 were determined by fitting the data to one-site saturation-binding curves.

Statistical analysis

Data are reported as means ± standard errors of the mean (SEMs). Differences between means at different time points before and after LCA ligation (a repeated measures analysis)

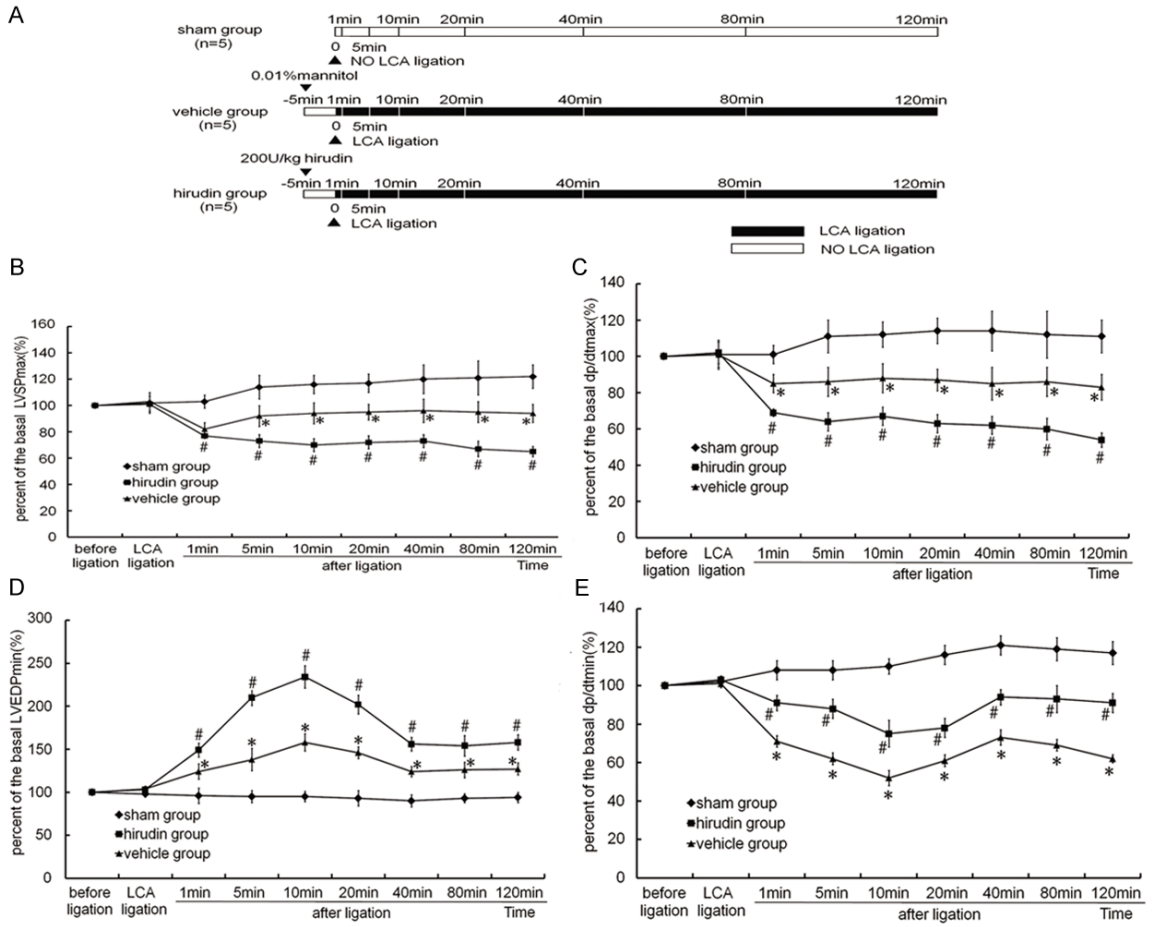

Figure 1. A: Experimental protocol. Sprague-Dawley rats were divided into three groups of five animals per group: sham group, hirudin group (200 U/kg), and vehicle group (0.01% mannitol). Hirudin or mannitol was injected into the right iliac vein 5 minutes before LCA ligation. The sham control involved an identical procedure, except that the LCA was not ligated. B and C: Percent changes in $LVSP_{max}$ and dp/dt_{max} from basal values at different time points in each group. D and E: Percent changes in LVEDP and dp/dt_{min} from basal values at different time points in each group. Data are shown as the mean ± SEM. *P < 0.05 for vehicle *vs*. sham group. #P < 0.05 for hirudin *vs*. sham group. Mannitol is the vehicle of hirudin.

were evaluated by using a linear mixed effects model with a random effect for each anima performed using SAS Statistical Software (version 9.2, SAS Institute Inc.). Differences between means, non repeated measures, were evaluated by analysis of variance (ANOVA) and Student's *t*-test (paired data, unpaired data, and multiple data sets). Differences with $P < 0.05$ were considered statistically significant.

Results

Effect of thrombin on cardiac function after AMI

To determine the influence of thrombin receptor activation on cardiac function after AMI, the right iliac vein was injected with 200 U/kg hirudin (to eliminate thrombin) or vehicle (0.01% mannitol) 5 minutes before LCA ligation (**Figure 1A**). Compared to vehicle treatment, hirudin decreased $LVSP_{max}$, dp/dt_{max}, and dp/dt_{min}, but increased LVEDP, from 1 to 120 minutes after AMI (**Figure 1B-E**). When TRAP (270 mM, 100 μL) was injected into the iliac vein 1 minute before LCA ligation, the hirudin-induced effect of decreased cardiac function was reversed (**Figure 2B-E**). With each intervention, the peak effect on LVEDP and dp/dt_{min} occurred around 10 minutes after AMI. The levels gradually recovered, but remained different from those of the sham control groups.

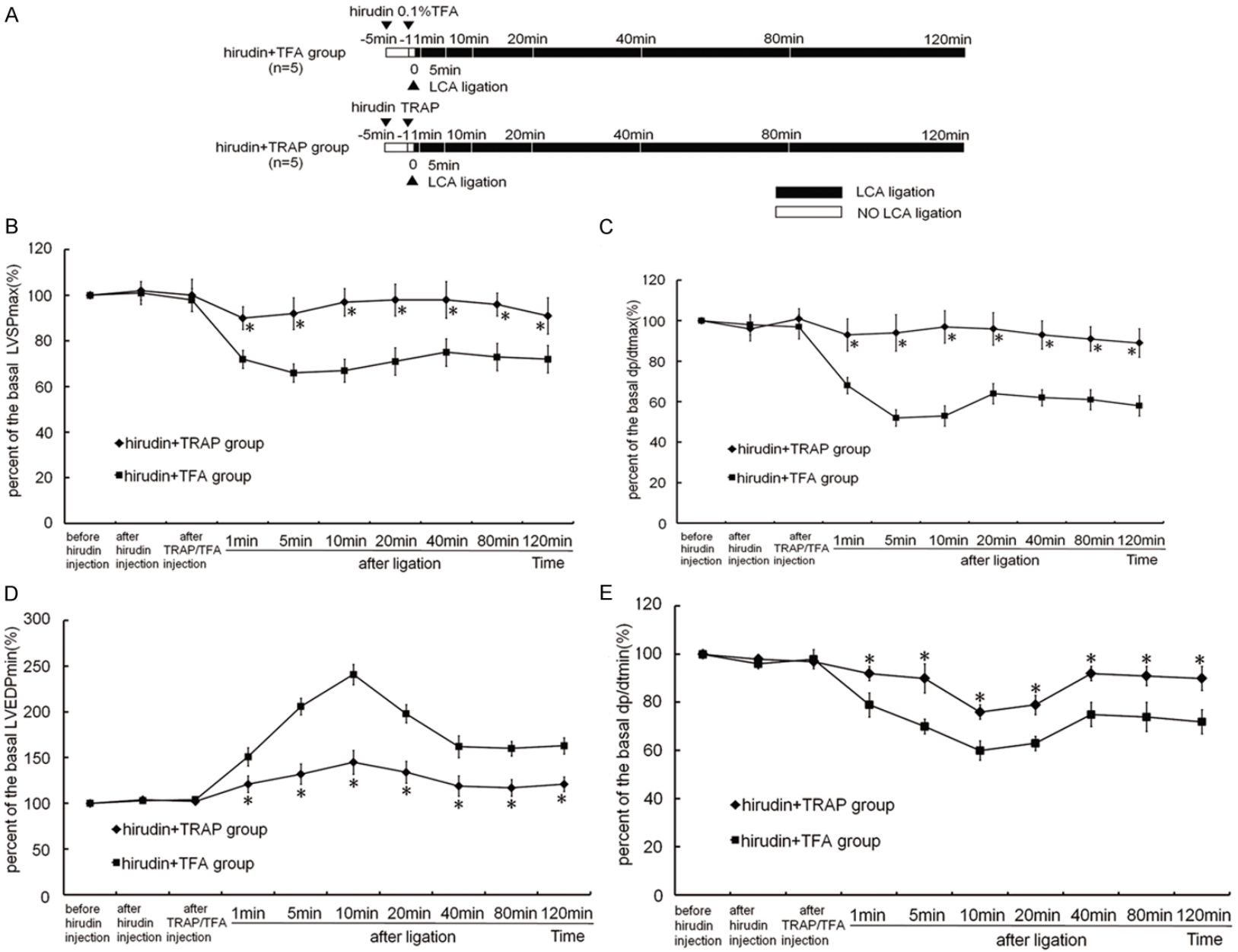
A
hirudin 0.1%TFA
-5min -1 1min 10min 20min 40min 80min 120min
hirudin+TFA group
(n=5)
0 5min
LCA ligation
hirudin TRAP
-5min -1 1min 10min 20min 40min 80min 120min
hirudin+TRAP group
(n=5)
0 5min
LCA ligation
LCA ligation
NO LCA ligation
B
percent of the basal LVSPmax(%)
hirudin+TRAP group
hirudin+TFA group
before hirudin injection
after hirudin injection
after TRAP/TFA injection
1min 5min 10min 20min 40min 80min 120min
after ligation
Time
C
percent of the basal dp/dtmax(%)
hirudin+TRAP group
hirudin+TFA group
before hirudin injection
after hirudin injection
after TRAP/TFA injection
1min 5min 10min 20min 40min 80min 120min
after ligation
Time
D
percent of the basal LVEDPmin(%)
hirudin+TRAP group
hirudin+TFA group
before hirudin injection
after hirudin injection
after TRAP/TFA injection
1min 5min 10min 20min 40min 80min 120min
after ligation
Time
E
percent of the basal dp/dtmin(%)
hirudin+TRAP group
hirudin+TFA group
before hirudin injection
after hirudin injection
after TRAP/TFA injection
1min 5min 10min 20min 40min 80min 120min
after ligation
Time

Figure 2. A: Experimental protocol. Sprague-Dawley rats were divided into two groups of five animals per group: hirudin + TFA and hirudin + TRAP. Hirudin was administered intravenously *via* the left iliac vein 5 minutes before LCA ligation, followed by TFA/TRAP injection 1 minute before LCA ligation. B and C: Percent changes of $LVSP_{max}$ and dp/dt_{max} from basal values at different time points in each group. D and E: Percent changes in LVEDP and dp/dt_{min} from basal values at different time points in each group. Data shown are the mean ± SEM. *P < 0.05 for hirudin + TFA *vs*. hirudin + TRAP group. TFA is the vehicle of TRAP.

Effect of hirudin on the expression of the IP_3R subtypes after AMI

Given the importance of IP_3 as a second messenger, we hypothesized that thrombin could exert its effects on cardiac function through IP_3R. Using RT-PCR and Western blot analyses, we measured the mRNA and protein expression levels, respectively, of IP_3R subtypes after neutralizing thrombin with hirudin in the infarct area. The results are shown in **Figure 3** (data are reported as the fold change relative to the basal level).

The mRNA expression levels of IP_3R-1, -2, and -3 in the hirudin group were less than those in the vehicle group at 5 minutes (2.64 ± 0.06, 1.54 ± 0.03, 3.21 ± 0.02 *vs*. 4.36 ± 0.03, 5.45 ± 0.02, 2.78 ± 0.02 folds), 10 minutes (3.13 ± 0.02, 2.12 ± 0.02, 4.24 ± 0.04 *vs*. 5.12 ± 0.03, 3.84 ± 0.01, 6.32 ± 0.01 folds), 20 minutes (2.78 ± 0.05, 1.46 ± 0.03, 3.22 ± 0.03 *vs*. 3.97 ± 0.04, 2.62 ± 0.06, 5.17 ± 0.04 folds), and 40 minutes after AMI (1.04 ± 0.02, 1.13 ± 0.01, 1.65 ± 0.06 *vs*. 1.62 ± 0.04, 2.11 ± 0.06, 3.26 ± 0.02 folds). The mRNA expression level of IP_3R-2 in the hirudin group was less than that in the vehicle group at 80 minutes (0.78 ± 0.02 *vs*. 1.32 ± 0.04 folds) and 120 minutes (0.62 ± 0.03 *vs*. 1.21 ± 0.01 folds) after AMI (**Figure 3B1-D1**). The hirudin and vehicle groups displayed no significant difference in the mRNA expression level of IP_3R-1 or -3 at 80 minutes (0.91 ± 0.03, 0.82 ± 0.05 *vs*. 1.24 ± 0.04, 1.22 ± 0.01 folds) or 120 minutes after AMI (1.02 ± 0.05, 0.78 ± 0.04 *vs*. 1.03 ± 0.02, 0.82 ± 0.05 folds).

Similar changes to those observed for the mRNA expression were also observed for the protein expression levels of IP_3R-1, -2, and -3 between the two groups (**Figure 3B2-D2**). Immunohistochemistry for the protein expression levels of IP_3R-1, 2, and 3 in cardiomyocytes in the infarct areas showed similar differences between the two groups to those observed for the protein and mRNA expression levels (Supplementary Figure 1A-C).

Effect of TRAP on the expression of the IP_3R subtypes after AMI

To clarify the relationship between IP_3R and the thrombin receptor, hirudin was injected into the iliac vein 5 minutes before LCA ligation, followed by 100 μl of 270 mmol/L TRAP or 100 μl of 0.1% TFA (the vehicle of TRAP) 1 minute before LCA ligation. Using RT-PCR and Western blot analyses, we measured the mRNA and protein expression levels, respectively, of the IP_3R subtypes in the infarct area. The results are shown in **Figure 4** (data are reported as the fold change relative to the basal level).

The mRNA expression levels of IP_3R-1, -2, and -3 in the hirudin + TFA group were less than levels in the hirudin + TRAP group at 5 minutes (2.12 ± 0.04, 1.98 ± 0.04, 2.56 ± 0.03 *vs*. 3.52 ± 0.02, 3.14 ± 0.02, 4.02 ± 0.07 folds), 10 minutes (3.01 ± 0.02, 2.51 ± 0.01, 3.12 ± 0.02 *vs*. 4.76 ± 0.03, 4.01 ± 0.02, 5.64 ± 0.05 folds), 20 minutes (2.14 ± 0.06, 1.86 ± 0.07, 2.23 ± 0.06 *vs*. 3.42 ± 0.02, 3.17 ± 0.03, 4.42 ± 0.04 folds), and 40 minutes after AMI (0.98 ± 0.02, 0.98 ± 0.06, 1.02 ± 0.03 *vs*. 2.14 ± 0.03, 1.66 ± 0.04, 2.04 ± 0.01 folds). The IP_3R-2 mRNA expression in the hirudin + TFA group was less than that in the hirudin + TRAP group at 80 minutes (0.83 ± 0.04 *vs*. 1.41 ± 0.02 folds) and 120 minutes after AMI (0.68 ± 0.01 *vs*. 1.22 ± 0.03 folds; **Figure 4A1-C1**). The two groups showed no significant difference in the IP_3R-1 or -2 mRNA expression at 80 minutes (0.92 ± 0.02, 0.88 ± 0.04 *vs*. 0.89 ± 0.02, 0.81 ± 0.07 folds) or 120 minutes after AMI (0.88 ± 0.03, 0.82 ± 0.01 *vs*. 0.84 ± 0.04, 0.79 ± 0.03 folds).

Changes in the protein expression levels of IP_3R-1, -2, and -3 between the two groups were similar to those observed for mRNA expression (**Figure 4A2-C2**). Similar to the protein and mRNA expression differences, immunohistochemistry showed the same differences between the two groups in the protein expression levels of IP_3R-1, 2, and 3 in cardiomyocytes from the infarct areas (Supplementary Figure 2A-C).

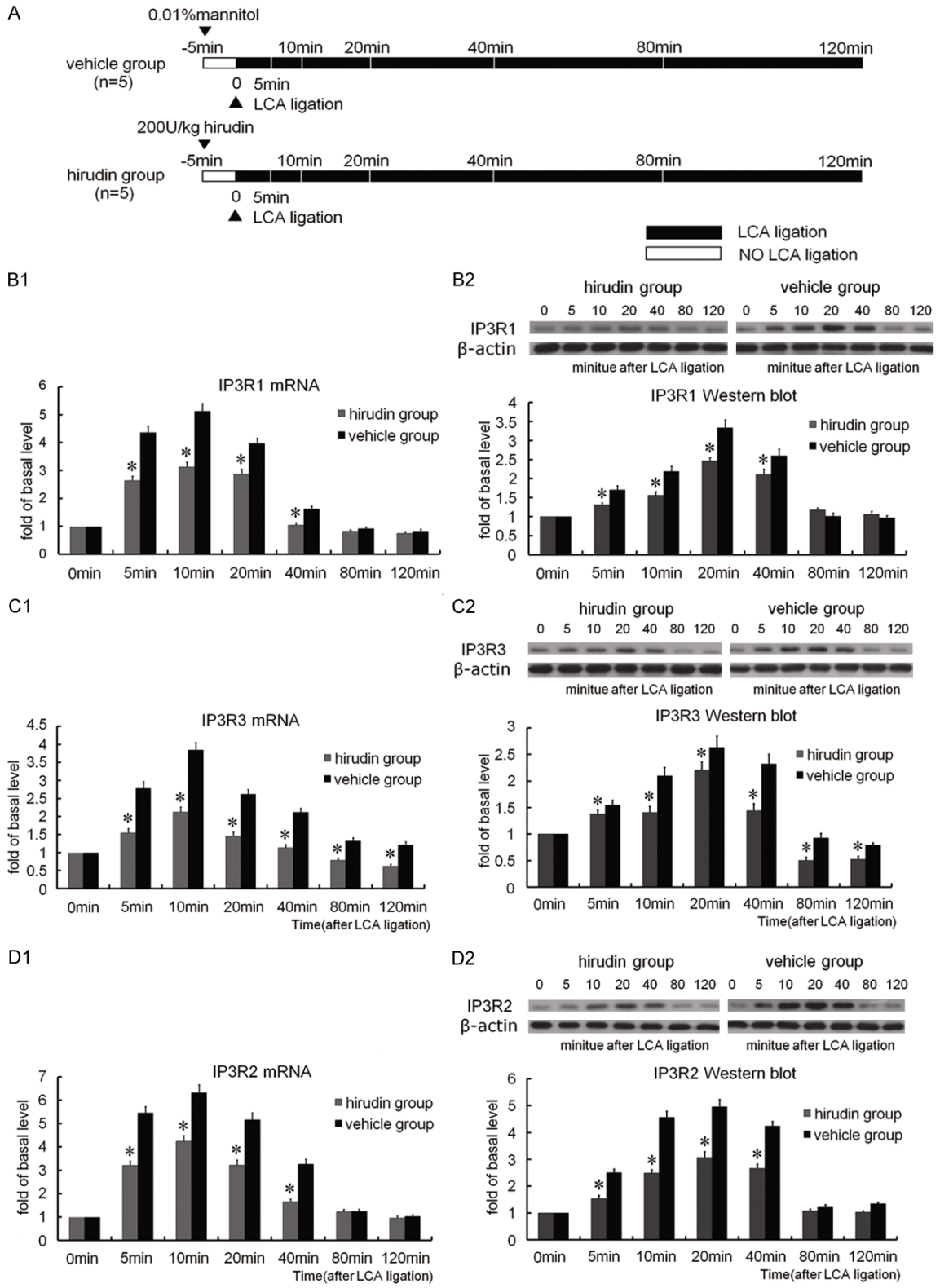

Figure 3. A: Experimental protocol. Sprague-Dawley rats were divided into two groups of five animals per group: vehicle and hirudin. Hirudin (200 U/kg) or 0.01% mannitol was injected into the right iliac vein before LCA ligation. B1, C1, and D1: Histograms showing the mRNA expression ratio of IP_3R-1, -2, or -3 relative to β-actin in the rat myocardium. Data (mean ± SEM) are expressed as a multiple of the basal level (fold), defined as the mRNA expression ratio at the LCA ligation time-point. *$P < 0.05$ for hirudin *vs*. vehicle group. B2, C2, and D2: Upper images show rep-

resentative Western blot analyses for IP_3R-1, -2, and -3 and β-actin protein expressions in the rat AMI myocardium at different time points after AMI. The three bottom histograms show the protein expression ratios of rat myocardium IP_3R-1, -2, and -3 relative to β-actin. Data (mean ± SEM) are expressed as a multiple of the basal level (fold), defined as the protein expression ratio at the LCA ligation time point. *P < 0.05 for hirudin *vs*. vehicle group. Mannitol is the vehicle of hirudin.

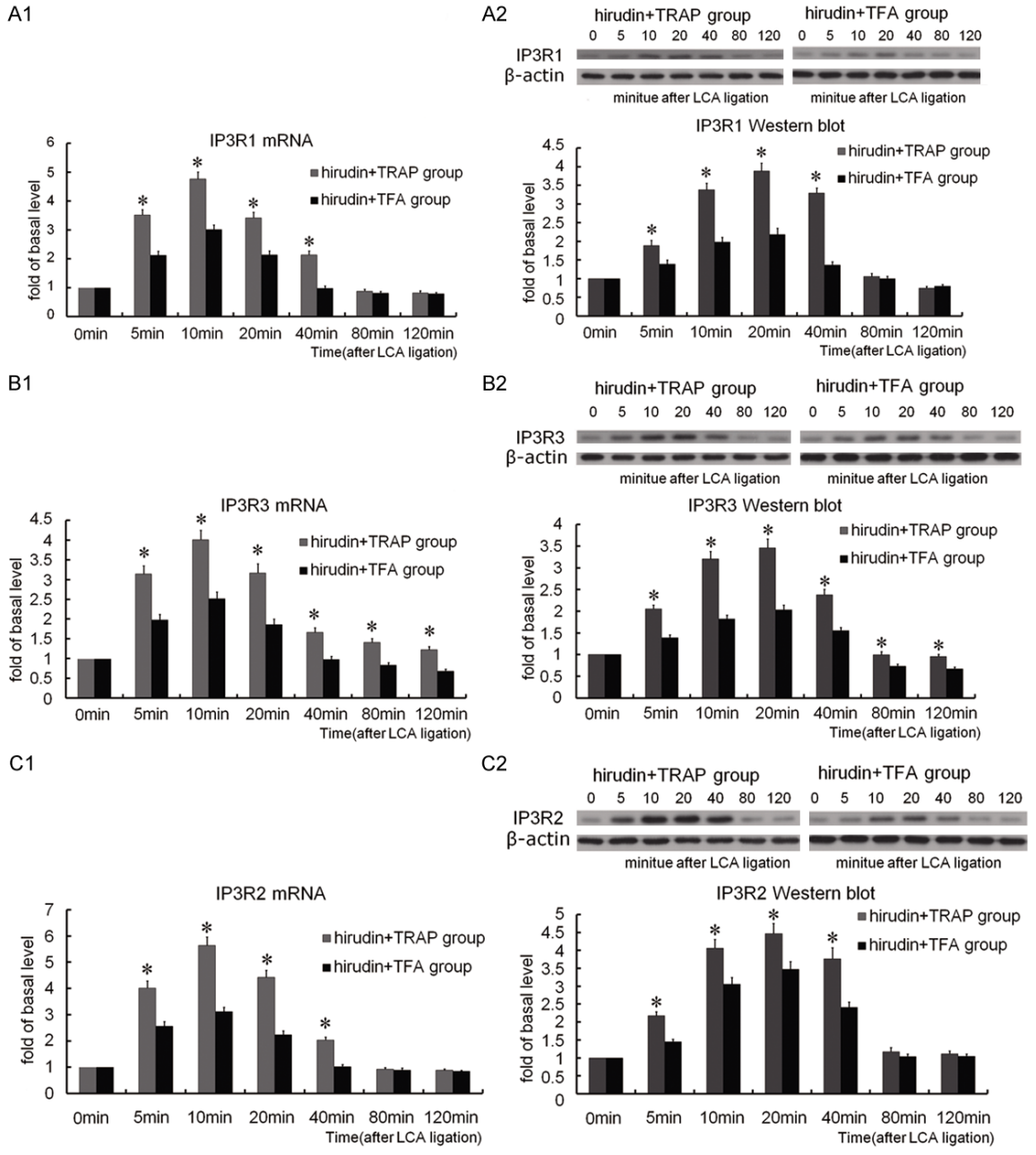

Figure 4. Same experimental protocol as **Figure 2A**. A1, B1, and C1: Histograms showing mRNA expression ratios of rat myocardium IP_3R-1, -2, and -3 relative to β-actin. Data (mean ± SEM) are expressed as a multiple of the basal level (fold), defined as the mRNA expression ratio at the LCA ligation time point. *P < 0.05 for hirudin + TRAP *vs*. hirudin + TFA group. A2, B2, and C2: Upper images show representative Western blot analyses for IP_3R-1, -2, and -3 and β-actin protein expression in rat AMI myocardium at different time points after AMI. Three bottom histograms show the protein expression ratios of rat myocardium IP_3R-1, -2, and -3 relative to β-actin. Data (mean ± SEM) are expressed as a multiple of the basal level (fold), defined as the protein expression ratio at the LCA ligation time point. *P < 0.05 for hirudin + TRAP *vs*. hirudin + TFA group. TFA is the vehicle of TRAP.

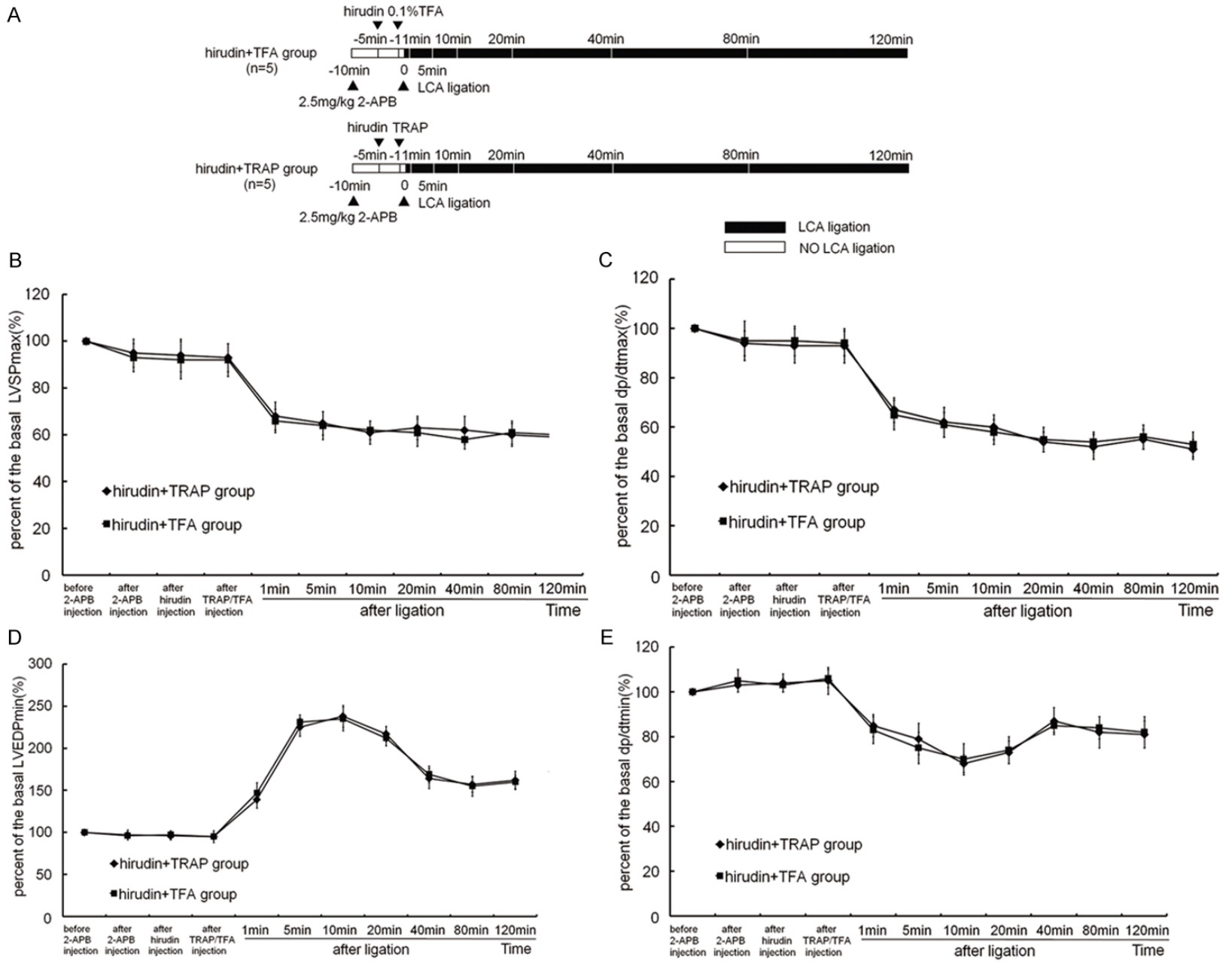
A
hirudin 0.1%TFA
-5min -1 1min 10min 20min 40min 80min 120min
hirudin+TFA group
(n=5)
-10min 0 5min
LCA ligation
2.5mg/kg 2-APB
hirudin TRAP
-5min -1 1min 10min 20min 40min 80min 120min
hirudin+TRAP group
(n=5)
-10min 0 5min
LCA ligation
2.5mg/kg 2-APB
LCA ligation
NO LCA ligation
B
percent of the basal LVSPmax(%)
hirudin+TRAP group
hirudin+TFA group
before 2-APB injection
after 2-APB injection
after hirudin injection
after TRAP/TFA injection
1min 5min 10min 20min 40min 80min 120min
after ligation
Time
C
percent of the basal dp/dtmax(%)
hirudin+TRAP group
hirudin+TFA group
before 2-APB injection
after 2-APB injection
after hirudin injection
after TRAP/TFA injection
1min 5min 10min 20min 40min 80min 120min
after ligation
Time
D
percent of the basal LVEDPmin(%)
hirudin+TRAP group
hirudin+TFA group
before 2-APB injection
after 2-APB injection
after hirudin injection
after TRAP/TFA injection
1min 5min 10min 20min 40min 80min 120min
after ligation
Time
E
percent of the basal dp/dtmin(%)
hirudin+TRAP group
hirudin+TFA group
before 2-APB injection
after 2-APB injection
after hirudin injection
after TRAP/TFA injection
1min 5min 10min 20min 40min 80min 120min
after ligation
Time

Figure 5. A: Experimental protocol. Sprague-Dawley rats were divided into two groups of five animals per group: hirudin + TFA, and hirudin +TRAP. 2-APB (2.5 mg/kg) or hirudin was administered intravenously *via* the iliac vein 10 or 5 minutes before LCA ligation, respectively, followed by TFA/TRAP 1 minute before LCA ligation. B and C: Percent changes in the $LVSP_{max}$ and dp/dt_{max} from basal values at different time points in each group. D and E: Percent changes in the LVEDP and dp/dt_{min} from basal values at different time points in each group. Data are shown as the mean ± SEM. *P < 0.05 for hirudin +TFA *vs*. hirudin + TRAP group. TFA is the vehicle of TRAP.

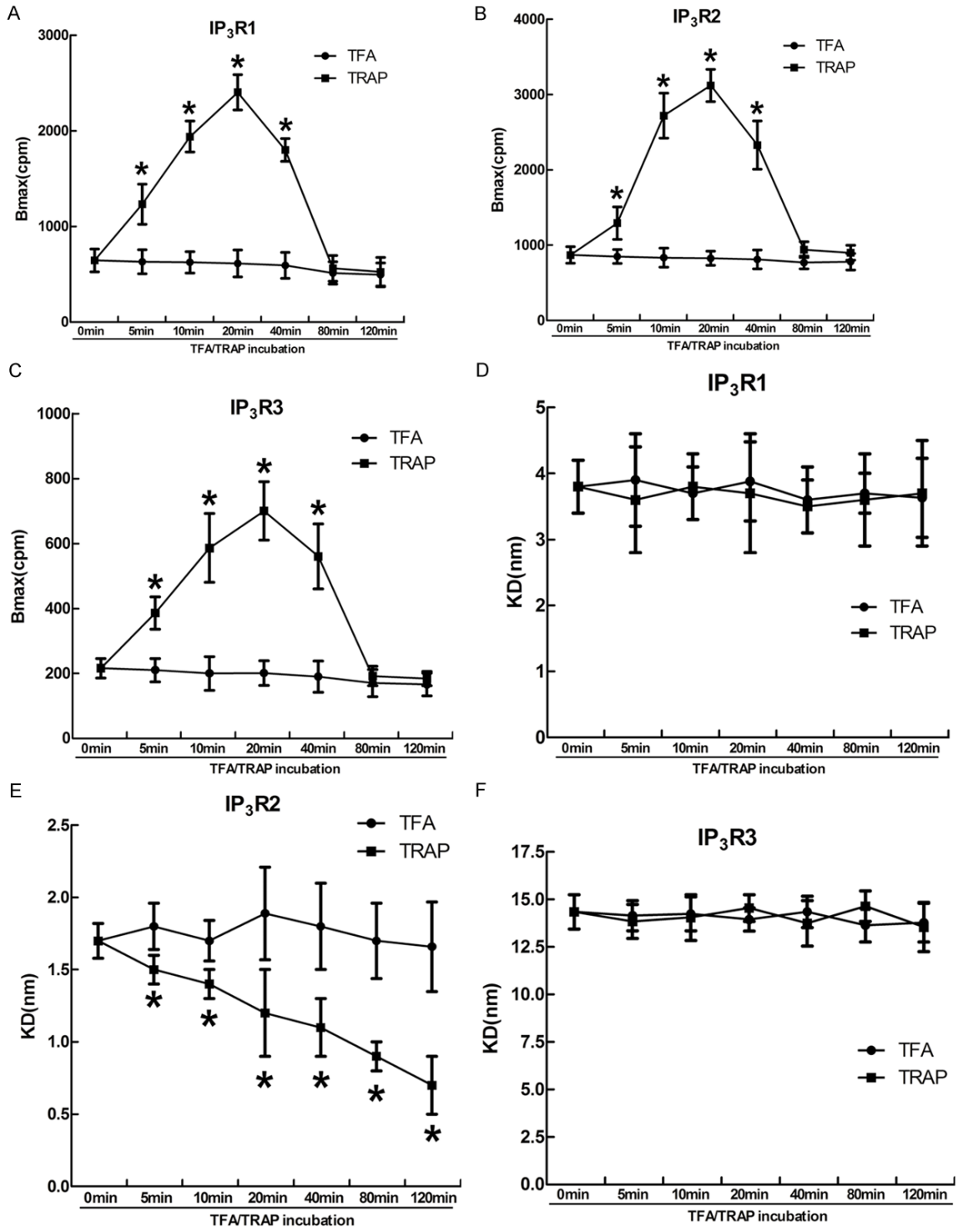

Figure 6. Effect of TRAP on the maximum binding capacity (B_{max}) and affinity (K_d) of IP_3R-1 (A and B), IP_3R-2 (C and D), and IP_3R-3 (E and F). Data are shown as the mean ± SEM (n = 5). *P < 0.05 at different time points of TRAP incubation *vs*. basal time point. TFA is the vehicle of TRAP.

Effect of 2-APB on cardiac function after AMI

To clarify whether the effect of thrombin on cardiac function is related to IP_3R, we used the IP_3R inhibitor, 2-APB. Treatment with 2-APB (2.5 mg/kg) in the hirudin + TRAP group eliminated the TRAP-induced improvement in the cardiac functional parameters ($LVSP_{max}$, dp/dt_{max}, LVEDP, and dp/dt_{min}) from 1 to 120 minutes after AMI compared to the hirudin + TFA group (P > 0.05, **Figure 5**).

Effect of TRAP on the affinity of IP_3 receptors in cardiomyocytes

As shown in **Figure 6**, the order of the basal affinity of the three subtypes of IP_3R in the TFA group was IP_3R-2 (1.8 ± 0.2 nM) > IP_3R-1 (3.9 ± 0.6 nM) > IP_3R-3 (14.1 ± 1.1 nM). The basal B_{max} values of IP_3R-1, -2, and -3 were 630 ± 115, 850 ± 150, and 210 ± 35 cpm, respectively. After incubation with TRAP for 20 minutes, the affinity of IP_3R-2 increased with time from 5 to 120 minutes compared to the basal TFA group (1.5 ± 0.3, 1.4 ± 0.1, 1.2 ± 0.3, 1.1 ± 0.2, 0.9 ± 0.1, and 0.7 ± 0.2 nM; P < 0.05), whereas the affinities of IP_3R-1 and -3 did not significantly change (IP_3R-1: 3.6 ± 0.8, 3.8 ± 0.5, 3.7 ± 0.9, 3.5 ± 0.4 , 3.6 ± 0.7, 3.7 ± 0.8 nM; IP_3R-3: 13.8 ± 0.9, 14 ± 1.2, 14.5 ± 0.7, 13.7 ± 1.2, 14.6 ± 0.8, 13.5 ± 1.3 nM). The B_{max} values of IP_3R-1, -2, and -3 increased with time from 5 to 40 minutes compared to the basal TFA group (1232 ± 210, 1940 ± 162, 2403 ± 185, 1800 ± 120 cpm; 1293 ± 216, 721 ± 300, 3123 ± 214, 2330 ± 320 cpm; and 386 ± 50, 586 ± 106, 700 ± 90, 560 ± 100 cpm, respectively; P < 0.05), but all of the values returned to their basal levels within 80 to 120 minutes after AMI (561 ± 135, 525 ± 150 cpm; 940 ± 104, 900 ± 98 cpm; and 192 ± 30, 184 ± 22 cpm, respectively; P > 0.05). These results also were illustrated by Scatchard analysis (**Figure 7**). TRAP had much stronger effects on the affinity of IP_3R-2 compared to IP_3R-1 and -3, and it had no effect on the B_{max} of IP_3R-1 or -3.

Discussion

By eliminating thrombin, hirudin aggravated the cardiac dysfunction after AMI and decreased the expression of IP_3R subtypes, especially IP_3R-2. On the other hand, by activating the thrombin receptor, TRAP reversed the hirudin-induced cardiac dysfunction after AMI and increased the expression of all IP_3R subtypes, especially IP_3R-2. The ability of TRAP to improve cardiac function disappeared when rats were pretreated with 2-APB, an IP_3R antagonist. These findings reveal that the activated thrombin receptor elicited its effects on cardiac function after AMI *via* IP_3R.

For all interventions, the peak effects on LVEDP and dp/dt_{min} occurred around 10 minutes after AMI. The levels gradually recovered, although not to the levels of the sham control group. Thus, the peak effects on LVEDP and dp/dt_{min} after AMI probably did not come from the interventions themselves, but from the hemodynamic measurement methods. For example, when the cannulation tube was inserted into the LV *via* the common carotid artery went through the aorta and caused aorta valvular regurgitation, which may be one reason for our observation. The different interventions that we used in our experiments may have enhanced this effect.

The protease-activated receptor (PAR) superfamily of seven transmembrane G protein-coupled receptors includes PARs 1 to 4. The thrombin receptor is PAR-1 [15]. There is no direct evidence to prove that PAR-1 can affect cardiac function, but there is some indirect evidence. In the heart, PAR-1 is expressed by cardiomyocytes and cardiac fibroblasts [16, 17]. PAR-1 expression was recently shown to be increased in the hearts of patients with ischemic and idiopathic dilated cardiomyopathy [18]. It was elevated in the LV in a mouse model of chronic heart failure [19]. *In vitro* studies using rat neonatal cardiomyocytes demonstrated that PAR-1 activation induced hypertrophy [17, 20]. PAR-1-dependent changes included increases in intracellular Ca^{2+}, protein content, cell size, and sarcomeric organization. Furthermore, activation of PAR-1 in cardiac fibroblasts induced cell proliferation [16]. Thrombin stimulates fibroblasts *via* activation of phospholipase C that hydrolyzes phosphatidylinositol 4,5-bisphosphate to IP_3 and diacylglycero [21], which act as

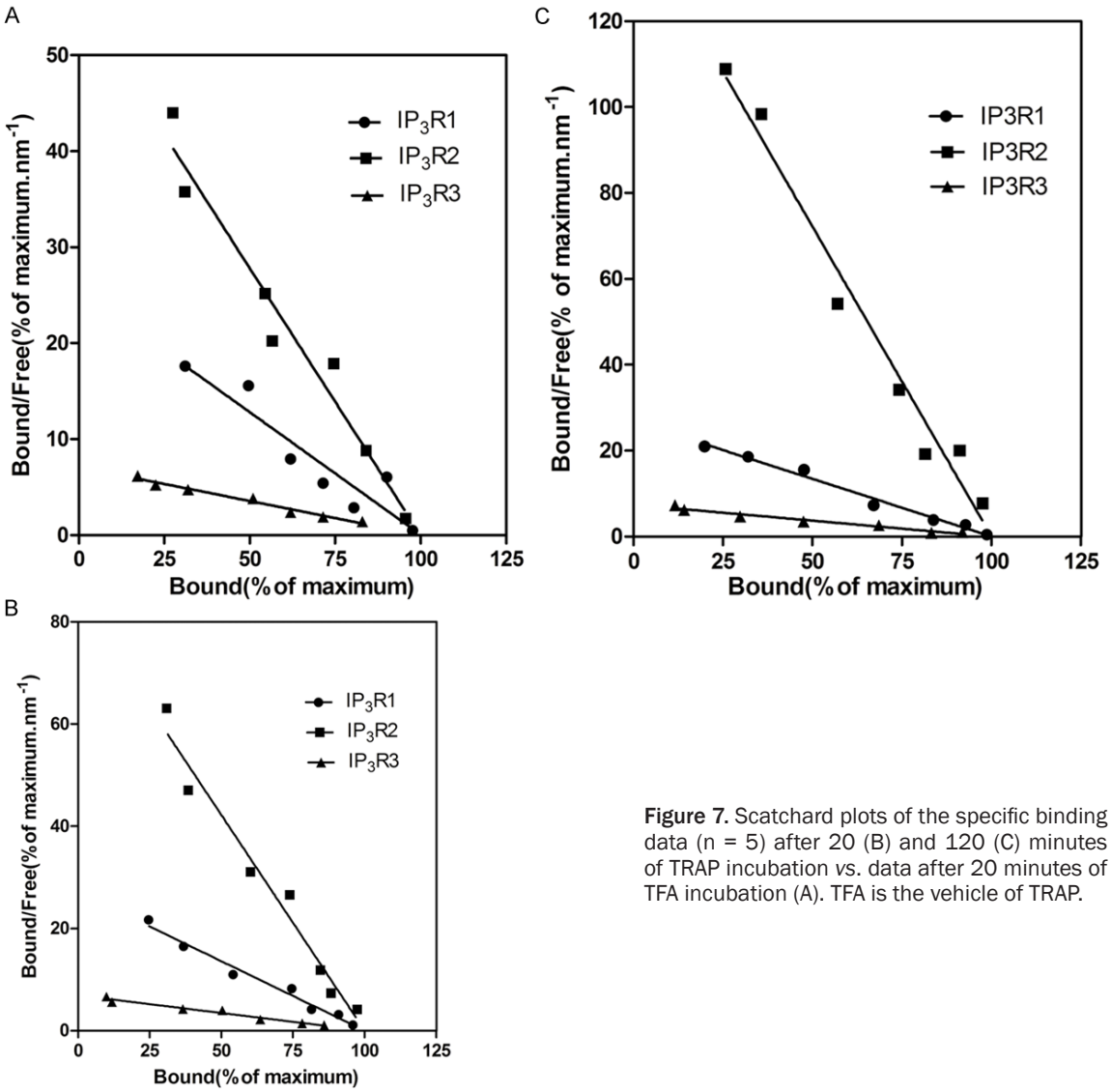

Figure 7. Scatchard plots of the specific binding data (n = 5) after 20 (B) and 120 (C) minutes of TRAP incubation *vs*. data after 20 minutes of TFA incubation (A). TFA is the vehicle of TRAP.

intracellular second messengers. In cardiomyocytes, PAR-1 results in IP_3R-mediated Ca^{2+} outflow from the SR and increased cytosolic Ca^{2+}, influencing cardiomyocyte contraction, electrophysiological changes, and the transcription of hypertrophy- and apoptosis-related nuclear factors [9]. IP_3 mobilizes Ca^{2+} from intracellular nonmitochondrial stores and elevates the intracellular Ca^{2+} concentration [22]. PAR-1 deficiency was shown to reduce LV dilation [23]. These results strongly suggest that PAR-1 may contribute to cardiac remodeling, which is the basis of heart functional changes, after injury [24]. However, PAR-1 has been reported to increase cardiac fibroblast proliferation and fibrotic activities [25]. Treatment with a PAR-1 inhibitor attenuated LV remodeling and infarct size in a rat myocardial ischemia-reperfusion model within 3 to 28 days after injury. The PAR-1 inhibitor did not cause any acute decrease in myocardial injury in the model [26, 27]. Our results prove that thrombin and PAR-1 activation improved cardiac function within 120 minutes. The improvement likely derived from the increased cardiac systolic function by PAR-1 activation, a phenomenon that is not unique for the thrombin receptor, one of G protein-coupled receptors. Indeed, activation of the β-adrenergic receptor, another one of G protein-coupled receptors, in the heart also acutely increases cardiac systolic function, but chronically stimulates LV remodeling in chronic heart failure and AMI. The latter effects are the basis for the broad clinical application of β-adrenergic recep-

tor blockers in chronical heart failure and AMI. One possibility is that PAR-1 temporarily compensates for the severely weakened neurohumoral regulation, which results from local blood and oxygen deficiencies in the infarcted area of the LV, for heart fuction after AMI.

Thrombin reportedly modulates phosphoinositide metabolism and cytosolic Ca^{2+} levels in the heart [28]. However, to the best of our knowledge, no study has reported that thrombin activation can induce improved cardiac function *via* IP_3R. PAR-1 activates signal transduction through a highly efficient process. Thrombin-activated myocardial cells generate IP_3 after 5 seconds, and the IP_3 level peaks within 1 minute [28]. Through its receptors, IP_3 elevates the intracellular Ca^{2+} concentration in the excitation-contraction coupling of cardiomyocytes, which is the basis of cardiac function. The increase in cytoplasmic free Ca^{2+}, resulting from increased IP_3 and IP_3R, is an important mechanism for regulating cardiac contractile forces in response to hormones and pharmacological factors. A greater than 2-fold increase of IP_3R mRNA in the heart was observed during end-stage heart failure in humans [29].

IP_3R subtypes 1, 2, and 3 are expressed in the heart [29]. IP_3R-1 is mainly found in nonmyocytes of human atrial tissue and in rat Purkinje cells [30, 31]. Most other species predominantly express IP_3R-2 in myocytes, with small amounts of IP_3R-1 and -3 [29, 30]. At the organelle level, IP_3R is mainly found in the SR around the ryanodine receptor in myocytes. IP_3R has been reported to mediate release of Ca^{2+} from other intracellular organelles, including the nuclear envelope [8], Golgi, and secretory vesicles [34, 35]. We found that all three IP_3R subtypes were expressed in the infarcted LV area, with IP_3R-2 being the most obvious . These findings are consistent with the previously reported literature.

Thrombin receptor activation induced IP_3R subtype changes within 40 minutes after AMI, although the effect of PAR-1 activation on cardiac function continued for more than 120 minutes. The effect of 2-APB on the TRAP-induced improvement in cardiac function also continued for more than 120 minutes. Most often, 2-APB is used as an experimental inhibitor of intracellular Ca^{2+} release through IP_3R [36, 37]. However, several reports have demonstrated that 2-APB affects the cell Ca^{2+} homeostasis in a concentration-dependent manner by depressing IP_3R activity and store-operated channel-linked Ca^{2+} entry at low concentrations [38, 39], while inducing Ca^{2+} leakage from isolated myocytes and nonexcitable cells at slightly higher concentrations [40]. Therefore, the effect of PAR-1 activation on cardiac function was not proven to occur through the IP_3R pathway. Since we can not find the same race of gene knockout animal (rat) and tried very hard with new techniques including miRNA and siRNA in cellular level, which did not give us convince data, so we have to conduct experiments to determine the effect of TRAP on the affinity of the IP_3R subtypes in cardiomyocytes because the IP_3R-mediated Ca^{2+} release from the endoplasmic reticulum is not only related to receptor expression and ligand number (B_{max}) but also to the IP_3R affinity. Thrombin receptor activation induced a change in the B_{max} values of all IP_3R subtypes for at least 80 minutes, but TRAP increased the affinity of the IP_3R-2 subtype for more than 120 minutes. As a result, the improvement in cardiac function by thrombin receptor activation might arise from the IP_3R-2 subtype.

In conclusion, thrombin and thrombin receptor activation improved cardiac function after AMI in rats. The improvement of cardiac function occurred through a pathway mediated by an IP_3R subtype (probably IP_3R-2).

Acknowledgements

This work was supported by the National Natural Science Foundation of China (No: 81170241 for Dr. Tang). We thank Mr. Dai Gang for his technical assistance with the animal model. We thank Drs. Zhang Jinxin and He Xianying from the Department of Biomedical Statistics of Public Health College of Sun Yat-Sen University for their assistance with statistical analysis.

Disclosure of conflict of interest

None to disclose.

Abbreviations

AMI, Acute myocardial infarction; TRAP, thrombin receptor-activating peptide; IP_3, inositol 1,4,5-trisphosphate; IP_3R, inositol 1,4,5-trisphosphate receptor; SR, sarcoplasmic reticu-

lum; TFA, trifluoroacetic acid; 2-APB, 2-aminoethoxydiphenyl borate; DMSO, dimethyl sulfoxide; LCA, left coronary artery; CCA, common carotid artery; LV, left ventricular; $LVSP_{max}$, LV systolic pressure; LVEDP, LV end-diastolic pressure; dp/dt_{max} and dp/dt_{min}, and the rise and fall rates in the LV pressure; DEPC, diethylpyrocarbonate; SDS, sodium dodecyl sulfate.

Address correspondence to: Dr. Jianping Zeng or Lilong Tang, Division of Cardiology, Xiangtan Central Hospital, #120 Heping Road, Xiangtan 411100, Hunan, PR China. Fax: + 86 20 873 30396; E-mail: zengjp88@163.com (JPZ); lilong_tang@yahoo.com (LLT)

References

[1] Babaev A, Frederick PD, Pasta DJ, Every N, Sichrovsky T, Hochman JS; NRMI Investigators. Trends in management and outcomes of patients with acute myocardial infarction complicated by cardiogenic shock. JAMA 2005; 294: 448-454.

[2] Goldberg RJ, Spencer FA, Gore JM, Lessard D, Yarzebski J. Thirty-year trends (1975 to 2005) in the magnitude of, management of, and hospital death rates associated with cardiogenic shock in patients with acute myocardial infarction: a population-based perspective. Circulation 2009; 119: 1211-1219.

[3] Loisance D. Editorial comment: Acute myocardial infarction and refractory cardiogenic shock: the simple, the better? Eur J Cardiothorac Surg 2013; 44: 217-218.

[4] Macfarlane SR, Seatter MJ, Kanke T, Hunter GD, Plevin R. Proteinase-activated receptors. Pharmacol Rev 2001; 53: 245-282.

[5] Leonardi S, Tricoci P, White HD, Armstrong PW, Huang Z, Wallentin L, Aylward PE, Moliterno DJ, Van de Werf F, Chen E, Providencia L, Nordrehaug JE, Held C, Strony J, Rorick TL, Harrington RA and Mahaffey KW. Effect of vorapaxar on myocardial infarction in the thrombin receptor antagonist for clinical event reduction in acute coronary syndrome (TRA-CER) trial. Eur Heart J 2013; 34: 1723-1731.

[6] Cheung WM, Andrade-Gordon P, Derian CK, Damiano BP. Receptor-activating peptides distinguish thrombin receptor (PAR-1) and protease activated receptor 2 (PAR-2) mediated hemodynamic responses in vivo. Can J Physiol Pharmacol 1998; 76: 16-25.

[7] Darrow AL, Fung-Leung WP, Ye RD, Santulli RJ, Cheung WM, Derian CK, Burns CL, Damiano BP, Zhou L, Keenan CM, Peterson PA, Andrade-Gordon P. Biological consequences of thrombin receptor deficiency in mice. Thromb Haemost 1996; 76: 860-866.

[8] Moschella MC, Marks AR. Inositol 1,4,5-trisphosphate receptor expression in cardiac myocytes. J Cell Biol 1993; 120: 1137-1146.

[9] Jiang T, Danilo P Jr, Steinberg SF. The thrombin receptor elevates intracellular calcium in adult rat ventricular myocytes. J Mol Cell Cardiol 1998; 30: 2193-2199.

[10] Tang lilong, Deng C, Long M, Tang A, Wu S, Dong Y, Saravolatz LD, Gardin JM. Thrombin receptor and ventricular arrhythmias after acute myocardial infarction. Molecular Medicine 2008; 14: 131-140.

[11] Long M, Yang L, Huang G, Liu L, Dong Y, Du Z, Tang A, Hu C, Gu R, Gao X, Lilong Tang. Thrombin and its receptor enhance ST-segment elevation in acute myocardial infarction by activating the KATP channel. Molecular Medicine 2010; 16: 322-332.

[12] Jaffré F, Friedman AE, Hu Z, Mackman N, Blaxall BC. β-adrenergic receptor stimulation transactivates protease-activated receptor 1 via matrix metalloproteinase in cardiac cells. Circulation 2012; 125: 2993-3003.

[13] Joseph SK, Samanta S. Detergent solubility of the inositol trisphosphate receptor in rat brain membranes. Evidence for association of the receptor with ankyrin. J Biol Chem 1993; 268: 6477-6486.

[14] Wojcikiewicz RJ, Luo SG. Differences among type I, II, and III inositol-1,4,5-trisphosphate receptors in ligand-binding affinity influence the sensitivity of calcium stores to inositol-1,4,5-trisphosphate. Mol Pharmacol 1998; 53: 656-662.

[15] Coughlin SR. Thrombin signalling and protease-activated receptors. Nature 2000; 407: 258-264.

[16] Sabri A, Short J, Guo J, Steinberg SF. Protease-activated receptor-1-mediated DNA synthesis in cardiac fibroblast is via epidermal growth factor receptor transactivation: distinct PAR-1 signaling pathways in cardiac fibroblasts and cardiomyocytes. Circ Res 2002; 91: 532-539.

[17] Sabri A, Muske G, Zhang H, Pak E, Darrow A, Andrade-Gordon P, Steinberg SF. Signaling properties and functions of two distinct cardiomyocyte protease-activated receptors. Circ Res 2000; 86: 1054-1061.

[18] Moshal KS, Tyagi N, Moss V, Henderson B, Steed M, Ovechkin A, Aru GM, Tyagi SC. Early induction of matrix metalloproteinase-9 transduces signaling in human heart end stage failure. J Cell Mol Med 2005; 9: 704-713.

[19] Moshal KS, Tyagi N, Henderson B, Ovechkin AV, Tyagi SC. Protease-activated receptor and endothelial-myocyte uncoupling in chronic heart failure. Am J Physiol Heart Circ Physiol 2005; 288: H2770-H2777.

[20] Glembotski CC, Irons CE, Krown KA, Murray SF, Sprenkle AB, Sei CA. Myocardial alpha-throm-

bin receptor activation induces hypertrophy and increases atrial natriuretic factor gene expression. J Biol Chem 1993; 268: 20646-20652.
[21] Raben DM, Yasuda K, Cunningham DD. Modulation of thrombin-stimulated lipid responses in cultured fibroblasts. Evidence for two coupling mechanisms. Biochemistry 1987; 26: 2759-2765.
[22] Berridge MJ, Irvine RF. Irvine, Inositol phosphates and cell signalling. Nature 1989; 341: 197-205.
[23] Pawlinski R, Tencati M, Hampton CR, Shishido T, Bullard TA, Casey LM, Andrade-Gordon P, Kotzsch M, Spring D, Luther T, Abe J, Pohlman TH, Verrier ED, Blaxall BC, Mackman N. Protease-activated receptor-1 contributes to cardiac remodeling and hypertrophy. Circulation 2007; 116: 2298-2306.
[24] Steinberg SF. The cardiovascular actions of protease-activated receptors. Mol Pharmacol 2005; 67: 2-11.
[25] Snead AN, Insel PA. Defining the cellular repertoire of GPCRs identifies a profibrotic role for the most highly expressed receptor, protease-activated receptor 1, in cardiac fibroblasts. FASEB J 2012; 26: 4540-7.
[26] Strande JL, Hsu A, Su J, Fu X, Gross GJ, Baker JE. SCH 79797, a selective PAR1 antagonist, limits myocardial ischemia/reperfusion injury in rat hearts. Basic Res Cardiol 2007; 102: 350-8.
[27] Sonin DL, Wakatsuki T, Routhu KV, Harmann LM, Petersen M, Meyer J, and Strande JL. Protease-Activated Receptor 1 Inhibition by SCH79797 Attenuates Left Ventricular Remodeling and Profibrotic Activities of Cardiac Fibroblasts. J Cardiovasc Pharmacol Ther 2013; 18: 460-475.
[28] Steinberg SF, Robinson RB, Lieberman HB, Stern DM, Rosen MR. Thrombin modulates phosphoinositide metabolism, cytosolic calcium, and impulse initiation in the heart. Circ Res 1991; 68: 1216-1229.
[29] Lipp P, Laine M, Tovey SC, Burrell KM, Berridge MJ, Li W, Bootman MD. Functional InsP3 receptors that may modulate excitation-contraction coupling in the heart. Curr Biol 2000; 10: 939-942.
[30] Yamda J, Ohkusa T, Nao T, Ueyama T, Yano M, Kobayashi S, Hamano K, Esato K, Matsuzaki M. Up-regulation of inositol 1,4,5 trisphosphate receptor expression in atrial tissue in patients with chronic atrial fibrillation. J Am Coll Cardiol 2001; 37: 1111-1119.
[31] Gorza L, Schiaffino S, Volpe P. Inositol 1,4,5-trisphosphate receptor in heart: evidence for its concentration in Purkinje myocytes of the conduction system. J Cell Biol 1993; 121: 345-353.
[32] Li X, Zima AV, Sheikh F, Blatter LA, Chen J. Endothelin-1-induced arrhythmogenic Ca^{2+} signaling is abolished in atrial myocytes of inositol-1,4,5-trisphosphate(IP3)-receptor type 2-deficient mice. Circ Res 2005; 96: 1274-1281.
[33] Bare DJ, Kettlun CS, Liang M, Bers DM, Mignery GA. Cardiac type 2 inositol 1,4,5-trisphosphate receptor: interaction and modulation by calcium/calmodulin-dependent protein kinase II. J Biol Chem 2005; 280: 15912-15920.
[34] Rizzuto R, Pozzan T. Microdomains of intracellular Ca^{2+}: molecular determinants and functional consequences. Physiol Rev 2006; 86: 369-408.
[35] Vazquez G, Wedel BJ, Bird GS, Joseph SK, Putney JW. An inositol 1,4,5-trisphosphate receptor-dependent cation entry pathway in DT40 B lymphocytes. EMBO J 2002; 21: 4531-4538.
[36] Maruyama T, Kanaji T, Nakade S, Kanno T, Mikoshiba K. 2-APB, a membrane-penetrable modulator of IP3-induced Ca^{2+} release. J Biol chem 1997; 122: 498-505.
[37] Wu J, Kamimura N, Takeo T, Suga S, Wakui M, Maruyama T, Mikoshiba K. 2-APB modulates kinetics of intracellular Ca^{2+} signals mediated by IP3-sensitive Ca^{2+} stores in single pancreatic acinar cells of mouse. Mol Pharm 2000; 58: 1368-1374.
[38] Peppiatt CM, Collins TJ, Mackenzie L, Conway SJ, Holmes AB, Bootman MD, Berridge MJ, Seo JT, Roderick HL. 2-Aminoethoxydiphenyl borate (2-APB) antagonises inositol 1,4,5-trisphosphate-induced calcium release, inhibits calcium pumps and has a use-dependent and slowly reversible action on store-operated calcium entry channels. Cell Calcium 2003; 34: 97-108.
[39] Nicoud IB, Knox CD, Jones CM, Anderson CD, Pierce JM, Belous AE, Earl TM, Chari RS. 2-APB protects against liver ischemia-reperfusion injury by reducing cellular and mitochondrial calcium uptake. Am J Physiol Gastrointest Liver Physiol 2007; 293: G623-G630.
[40] Bootman MD, Collins TJ, Mackenzie L, Roderick HL, Berridge MJ, Peppiatt CM. 2-Aminoethoxyphenylborate (2-APB) is a reliable blocker of store-operated Ca^{2+} entry but an inconsistent inhibitor of InsP3-induced Ca^{2+} release. FASEB J 2002; 16: 1145-1150.

Supplement method

Immunohistochemistry of IP3R in the infarct area

Immunostaining of IP_3Rs in the infarct area from LV was used a modification of a previously described method [10]. Briefly, thin paraffin sections (5 μm) were deparaffinized with xylene, immediately immersed in acetone, and washed in PBS (pH 7.4). The sections were blocked with 5% bovine serum albumin at 4°C for 60 min and then incubated with anti-IP_3Rs primary antibody (Santa Crutz Biotech, Santa Crutz, CA, USA) for 60 min at 4°C. Immunolabeling was amplified with the avidinbiotin-peroxidase complex (ABC) method (Vectastin Kits; Vector Laboratories, Burlingame, CA, USA) and visualized by reaction with DAB.

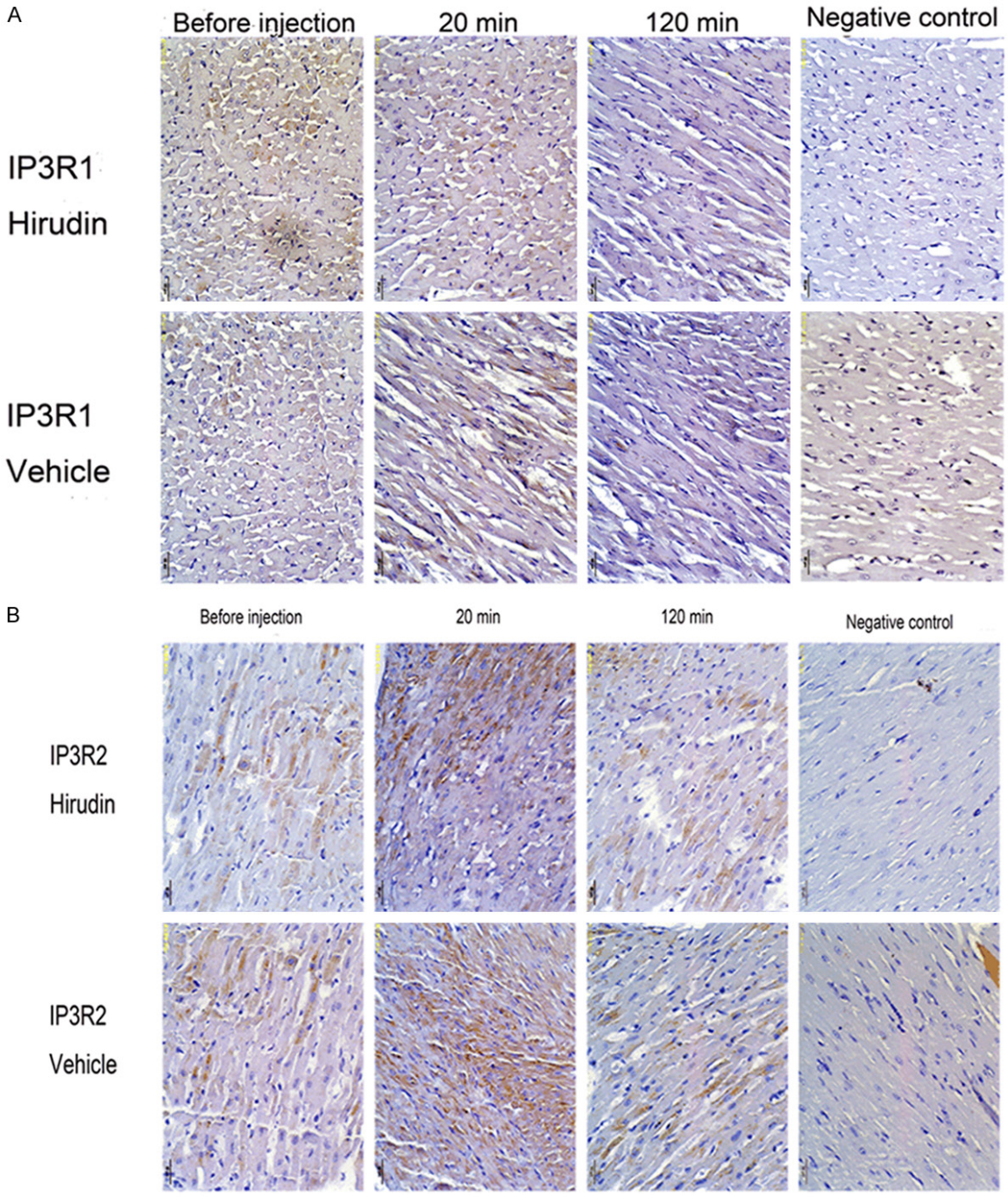

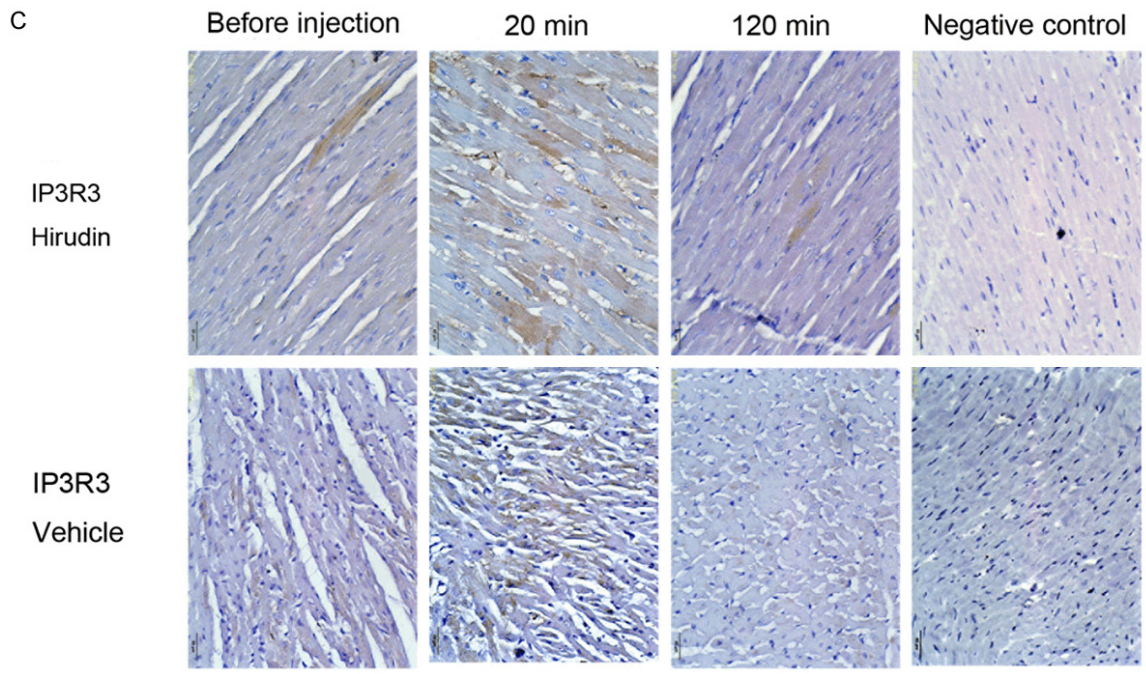

Supplementary Figure 1. A-C. Representative immunostaining for IP_3Rs in infarcted left ventricles at different time points. The same experimental protocol as **Figure 3**. These experiments showed the changes of IP_3 receptor 1, 2, and 3 expression located in cardiomyocytes from infracted left ventricles.

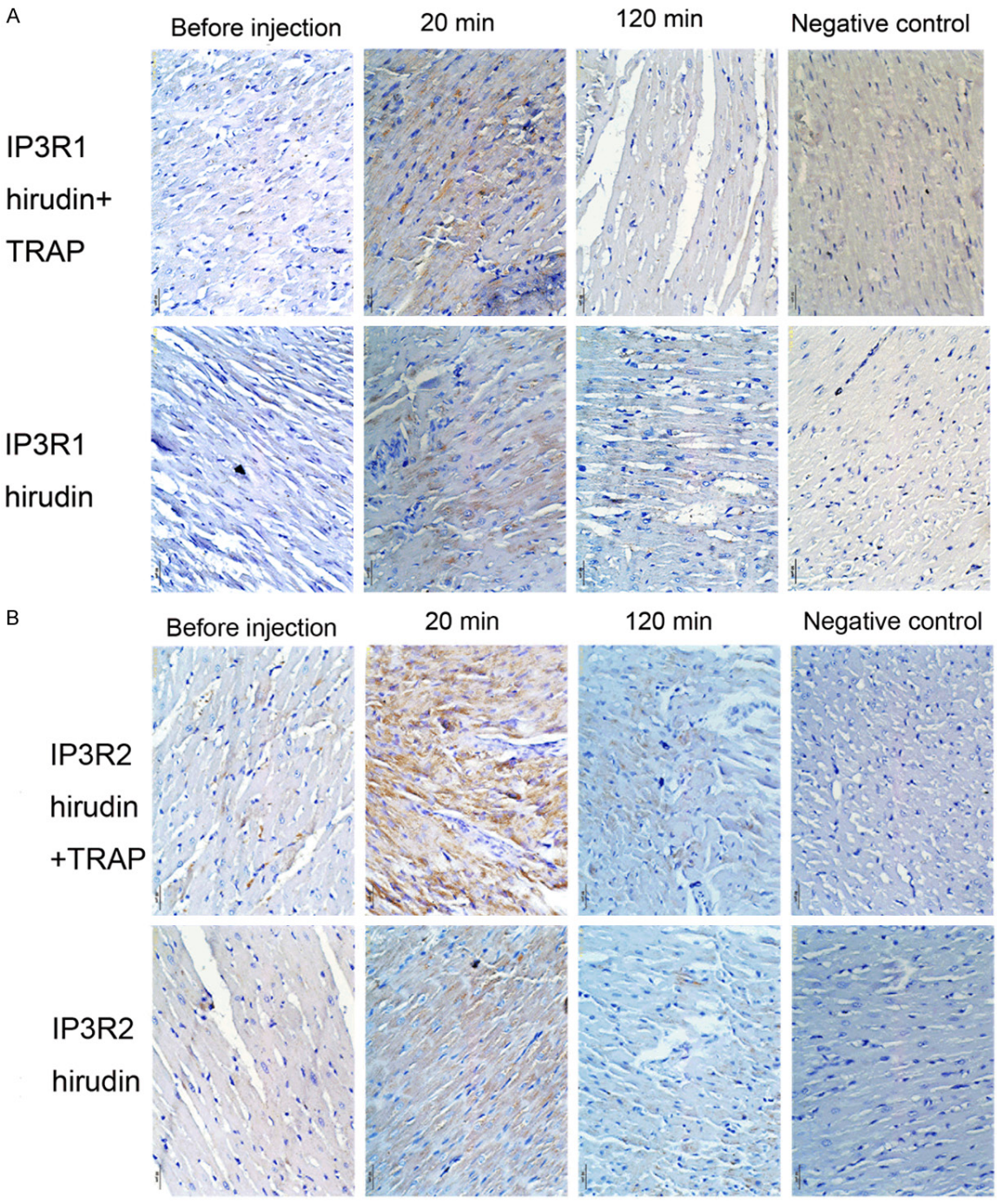
A
Before injection
20 min
120 min
Negative control
IP3R1
hirudin+
TRAP
IP3R1
hirudin
B
Before injection
20 min
120 min
Negative control
IP3R2
hirudin
+TRAP
IP3R2
hirudin

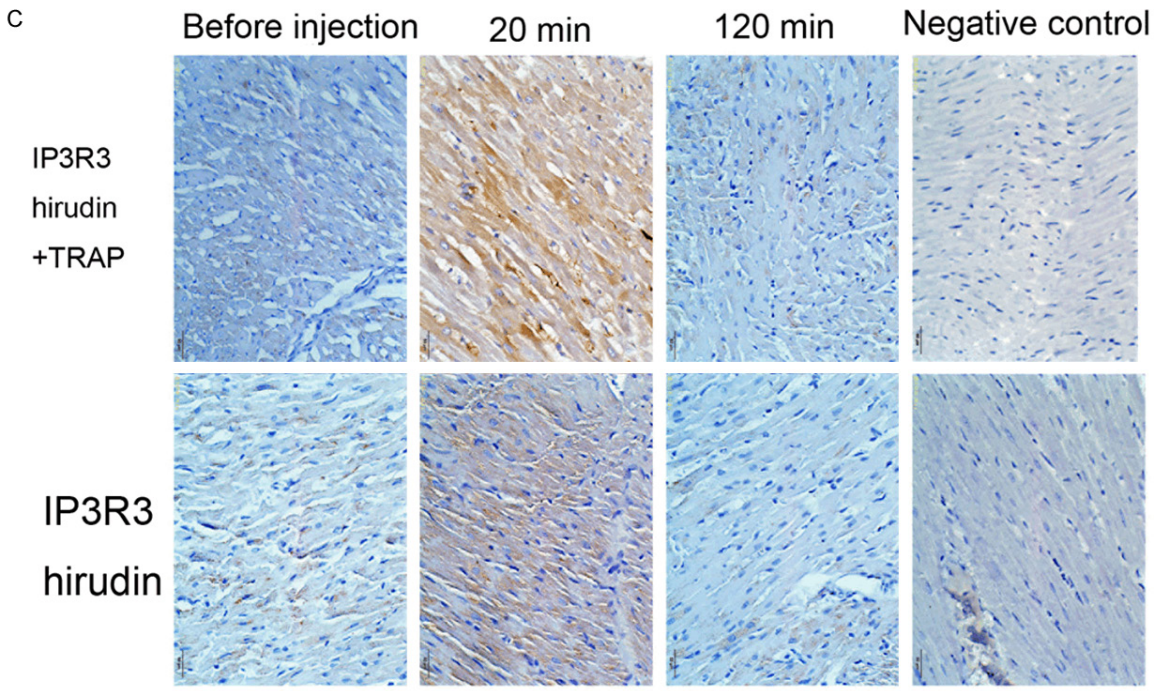

Supplementary Figure 2. A-C. Representative immunostaining for IP_3Rs in infarcted left ventricles at different time points. The same experimental protocol as **Figures 2** and **4**. These experiments showed the changes of IP_3 receptor 1, 2, and 3 expression located in cardiomyocytes from infracted left ventricles.